Approved For Release
2009/08/26 :
CIA-RDP88-00904R000100110

Third United Nations International Conference on the Peaceful Uses of Atomic Energy

A/CONF.28/P/367
USSR
May 1964
Original: RUSSIAN

Confidential until official release during Conference

EXPERIMENTAL STUDIES ON NEUTRON THERMALIZATION

By V.I.Mostovoy, V.S.Dykarev, I.P. Eremeev, S.P. Ishmayev, I.P. Sadikov, Yu. S. Saltykov, V.A.Taraban'ko, A.A.Chernyshov ↑ coded

Introduction

The experimental studies on neutron thermalization were initiated in Kurchatov IAE in the period when physical grounds of the projects of uranium-water reactors were being investigated. The physics of these reactors is known to be determined essentially by the space-energy distribution of thermal and epithermal neutrons (1). Meanwhile the calculation of the neutron spectra in heterogeneous uranium-water system was a difficult problem in this early time. Not only the effective methods of calculation were still to be developed. One had also to obtain the initial data on the neutron cross-sections to be input into calculations. This problem was especially difficult from the theoretical and experimental points of view for the double differential scattering cross-section of slow neutrons on the water. In this connection the initial experiments on the neutron thermalization consisted of the measurements of the neutron space-energy distributions in the uranium-water systems. Later such measurements were also carried out in the heterogeneous systems containing uranium with other moderators of interest for power reactors.

The results of these investigations made possible the determination of principal rules of space-energy distributions of neutrons in the heterogeneous systems and allowed to clear up the effects of chemical binding of moderator atoms on this distribution and the way in which the absorption acts upon it. The results were found to be useful for the estimation of the accuracy of approximate methods applied to the solution of the kinetic equation for the heterogenous systems and for the verification of various models describing the energy exchange between the neutron and moderator in the chamical binding energy range.

The research program on the neutron thermalization was expanded essentially in the direction of a more profound investigation of the laws obtained. Another object was clearing out the role of the absorption and the chemical binding in the formation of spectra in various systems.Now

[illegible] main directions:

1) study of double differential cross-sections for moderators in the thermal region of neutron energy;

2) study of the spectra of thermal and epithermal neutrons in various multiplying and moderating media;

3) study of the process of time thermal neutron spectrum setting up.

The results of these studies obtained in the last years are summarized in this report, and experimental technique is also briefly outlined.

I. Measurements of Double Differential Scattering Cross-Sections

Double differential scattering cross-sections $\sigma(E,E',\theta)$ were measured for water (H_2O) at T = 23°C and 90°C and monoisopropyldiphenyl ($C_{15}H_{16}$) at T = 20°C.

The experiments on the double differential cross-sections studies were carried out on the horizontal thermal neutron beam of the "WWR-M"-reactor of the Institute of Physics of the Academy of Sciences of the Ukrainian SSR.

I. Measurement Technique

Pulsed flux of "monochromatic" neutrons of energy E bombarding the moderator sample was separated from the thermal neutron beam by the mechanical monochromator with parabolic splits (Fig.1). The resolution of the monochromator did not depend on its revolution velocity and was equal to $\left(\frac{\Delta E}{E}\right)_{1/2} = 0.2$. The energy E^1 of neutrons scattered from the sample by angle Θ was measured by time-of-flight method with resolution 10 ÷ 40 μsec/m. The scattered neutrons were recorded by the assembly of BF_3 counters, located at a flight-distance L = 2.74 m. Effective dimensions of the detector were 30 x 60 x 10 cm. The measurements of the parameters examined were possible in following ranges of variables:

energy E from 5.10^{-3} to 0.5 ev
energy E^1 from 5.10^{-3} to 1.0 ev
angle Θ from 15° to 120°

The samples used in these measurements scattered ~ 20% of the total number of incident neutrons.

No corrections accounting the effects of resolution and multiple scattering were introduced into the double differential cross-sections because insufficient accuracy and uncompleteness of experimental data did not prove to be worth this laborious work.

2. Results

The variation of the double-differential cross-section $\sigma(E, E', \theta)$ is illustrated in Fig.2.

Being alike in general, double differential scattering cross-sections of water and monoisopropyldiphenyl differ in some details, reflecting the differences in the motion dynamics of hydrogen atoms and moleculed in these fluids. The value of quasielastic scattering peak in comparison with water is higher for monoisopropyldiphenyl, the width being consequently smaller almost for all scattering angles and incident neutron energies. These data indicate both a more hard binding of hydrogen in monoisopropyldiphenyl and a less diffusion coefficient of monoisopropyldiphenyl molecules in the fluid. The conclusion about diffusion coefficient is very natural because the molecule $C_{15}H_{16}$ has essentially larger mass than the water molecule.

In the inelastic scattering region cross-section values for these two liquids are very close. The energy region $E - E^1 \sim 60$ Mev is an exception, the difference, connected with excitation of braked rotations of the water molecules being very distinct in this region.

From the measured values of $\sigma(E, E', \theta)$ the mean energy variation in scattering $\bar{\varepsilon}$ (Fig.3a) and mean cosine of the scattering andle μ (Fig.3) were calculated. It is obvious that thermalization properties of $C_{15}H_{16}$ are worse than those of the water, but the angular neutron distribution in scattering is more isotropic.

The results obtained for the water sample heated up to 90°C indicate that the quasielastic scattering peak amplitude decreases and widens with temperature increasing. It may be due to the increasing of the diffusion coefficient and loosening of intermolecular bonds.

The probability of neutron scattering when neutrons gain energy increases with temperature rising.

All the information on the measurement results obtained for the water and monoisopropyldiphenyl is presented in Tables I and II in the form of the scattering law $S(\alpha, \beta)$ which reflects the effects of bonds and structure of the moderator itself on the scattering cross-sections (2). Experimental data are also presented in the form of generalized freqyency spectra $P(\beta)$ (Fig.4) according to Egelstaff and Scofield (3.4).

The generalized frequency spectrum contains very valuable information about atomic motion in the molecule and molecular motion in the fluid. Unfortunately, insufficient resolution and restricted accuracy did not allow to find out the detailed structure of these spectra.

However, even rather schematical outline of the generalized spectrum obtained for $C_{15}H_{16}$ shows its marked difference from the spectrum in the water. In the water at the room temperature the shape of the generalized spectrum is determined mainly by the interaction of the neutrons with the braked rotation of the water molecules. The level of the braked rotation is rather broad and is located at energy 65 MeV (2.5 β). This level shifts towards lower energies with increasing of water temperatures in qualitative agreement with the result given in papers [5] and [6] . Physical grounds of this phenomenon are not investigated yet. One of possible and natural reasons of this shift may be the loosening of intermolecular bonds with increasing of water temperature. The level shift may also be the consequence of more complicated structure of this level, including not only the braked rotation but other types of motion as well (5).

There is no broad level typical for the water at $\beta \simeq 2.5$ in the generalized frequency spectrum of $C_{15}H_{16}$ as can be seen in Fig.4. The mean energy of this spectrum is less than that of the water spectrum.

The obtained generalized frequency spectrum $\rho(\beta)$ makes it possible to calculate $\sigma (E, E', \theta)$ for any values of variables. These calculations are carried out in paper (7) for the water at the room temperature. $P (\beta)$ curve shown in Fig. 4a. was used in these calculations with three deltafunctions added reflect the well-known intrinsic molucular vibrations in the water. The results of the double differential cross-section calculations as well as average scattering characteristics $(\bar{\mu}(E), \bar{\xi}, \bar{\xi^2}, \bar{\xi})$ agree with the results of the present paper.

II. Stationary Neutron Spectra Measurements in Moderating and Multiplying Media

I. Measurement Technique

The measurement technique used for the measurements of neutron spectra was described in detail in papers [8,9] . It uses the beams of neutrons taken from the system under examination. The spectra of these beams are measured by the time-of-flight method with a mechanical chopper. The neutron spectra were investigated in the water with boron and in subcritical heterogeneous systems with natural uranium slugs. In these systems the external beams parallel to the slug axis were used. The required neutron density in the investigated systems was formed as a result of the irradiation with the broad beam of thermal of fast (converted from thermal) neutrons of "VVR-2"-reactor.

The measured spectra presented vector flux neutron spectra in the direction of the external beam. These measurements are in general insufficient for obtaining the scalar flux spectrum of practical value. However, the data on the spectra of vector flux neutrons obtained for one direction in the homogeneous medium permit to calculate easily the scalar flux spectrum in the diffusion approximation.

2. Results of Measurements

a) Neutron spectra in pure water and in water poisoned by boron.

The neutron spectra shown in Fig.5 were measured in pure water and in the water poisoned by boron (tank with dimensions 60 x 60 x 50 cm) at a distance 10.4 cm from the source of fast neutrons.

The spectrum hardens with increasing of boron concentration: the maximum of thermal neutron distribution shifts towards the higher energies and its value decreases as compared to the flux of slow neutrons.

The calculations of neutron spectra in the boron poisoned water for the concentrations used in our experiment were carried out by G.I. Marchuk et al [10] with the chemical binding of hydrogen in the water taken into account and by I.I.Laletin on the gas model with mass equal to unity. The calculation connected with more realistic conditions of energy exchange between the neutron and moderator obviously results in better agreement with experiment.

A number of experimental works on the investigation of neutron spectra in pure water and in water poisoned by various absorbers have been carried out up to date [11, 12, 12, 14, 15, 16] . The experimental conditions were different in this work as to the temperatures and concentrations. Because of it one of the possible ways for comparison of results of various works is to compare the dependence of the relative increase of neutron gas temperature on the absorber concentration (Fig.6. In this figure the well known dependence is shown

$$\frac{T_n - T_c}{T_n} = A \frac{\xi_a}{\xi \Sigma_s} \qquad (2)$$

with coefficients A = 1.84 according to gaseous moderator model [17] and A = 2.92 according to [10] . Though the experimental points show considerable spread, but A value given in [10] seems to be in better agreement with the experiment.

b) Neutron spectra in uranium-water lattice

The subcritical heterogeneous uranium-water systems were examined with triangle lattices with lattice spacing 5.0 cm, 5.5 cm and 6.0 cm

and subcritical uranium-monoisopropyldiphenyl heterogeneous system with the lattice spacing 5.5 cm. The natural uranium slugs 3.5 cm in diameter were used.

The experimental results have been published earlier [8, I8], and now we present only the main conclusions. The thermal neutron spectrum both in the lattice fuel cell and in the moderator, differs appreciably from equilibrium Maxwellian distribution. The neutron spectrum in the moderator may be approximately presented by the Maxwell form, but with "temperature" being essentially higher the temperature of the medium. The main condition determining the thermal neutron spectrum in the slug is the absorption of neutrons escaping from the water.

Neutron spectrum varius slightly with the spatial coordinate both in the fuel and moderator, the boundary between them being the only exception, where the spectrum changes sharply.

The spectrum of neutrons slowing down in the uranium slug bears the clear resonance structure determined by neutron absorption at the levels of U^{238} and U^{235}. In Fig. 7 the neutron spectrum in uranium measured with the resolution 1.2 $\mu sec/m$ in the lattice with spacing 5.5 cm in the energy region above 0.2 eV. The real shape of the spectrum above 20 eV is altered essentially by insufficient resolution of the selector. The spectrum in this region may be in principal reformed by the method proposed by A.N.Tikhonov (I9).

It should be noted that it is possible to obtain the value of neutron resonance absorption in the slug, calculating the area between spectral curves in uranium and moderator. This value may be obtained in principal for any energy interval.

The spectrum of the neutrons slowing down in the water, measured with the same resolution is close to the 1/E (Fig.8).

The results of thermal neutron spectra measurements in the lattice $C_{I5}H_{I6}$ with spacing 5.5 cm show the main laws of neutron space-energy distribution in the uranium-monoisoprpyldiphenyl lattice are the same as in uranium-water lattices. Thermalization properties of monoisopropyldiphenyl slightly differ from the water. The ranium-monoisopropyldiphenyl lattice is equivalent to the water lattice with a less spacing. The study of temperature dependence of the neutron spectra in the uranium monoisopropyldiphenyl lattice allows to make conclusions that the slowing properties of the monoisopropyldiphenyl slightly changes with temperature.

The changes of the neutron spectrum in the water with uranium concentration for the investigated uranium-water lattices are qualitively illustrated in Fig.9.

The neutron spectra in uranium-water lattices were calculated by a number of authors on the basis of various model assumptions about the nature of energy exchange between the neutron and the water molecule L.Sobrino and Clark (20) carried out the calculation of the neutron space-energy distribution using Wilkins-equation with γ-leakage thaken into account.

Their results are in good agreemnt with the results we obtained for the uranium-water lattice with the spacing 5.0 cm. H.Honek and H.Takahashi [21] have calculated the spectra of vector flux neutrons in various lattices. The calculations do not well agree with the results [22] and with our measurements for lattices with spacings 5 cm and 6 cm.

Recently G.I.Marchuck, V.V.Smelov and G.A.Ilyasova [23] carried out the calculation of the vector flux neutron spectra in uranium-graphite lattice with spacing 5.5 cm. The neutron-spactra were computed in P_3-approximation by using the scattering function proposed by Van Hove. The dispersion of autocorrelation function was found by the application of interpolation formulae proposed by V.F.Turchin. The agreement between the theory and experiment is good for the spectrum in the water on the boundary of the cell [18] . It should be noted that the calculated neutron spectra in water on the cell boundary practically do not show any angular anisotropy. The spectra of vector flux neutrons, computed for the directions parallel and perpendicular to the slug axis differ considerably (Fig.10). Experimental points lay between the spectrum calculated for the parallel direction and the spectrum of scalar flux closer to the latter.

Campbell et al (22) investigated the neutron spectra in the ecternal beams from the uranium slugs and from the water in the directions parallel and perpendicular to the slug axis. It should be noted, that the results of calculations (23) predict an essentially less value of the spectrum anisotropy in the slug and practically no anisotropy in the moderator for the lattices examined.

c) Uranium-Graphite Lattice

The neutron spectra were examined in the cell of the subcritical uranium-graphite lattice of the Calder Hall type at various graphite temperatures (lattice spacing 20 cm, diameter of natural uranium blocks 3.5 cm). The dimensions of the subcritical assembly were 120x120x120 cm^3. The uranium slugs covered by aluminium were placed in the special channels and isolated from graphite by the air gap. The volume concentrations of uranium, graphite, aluminium and air were

equal to 0.096; 0.834; 0.021; 0.049 respectively.

Nuclear power and electric heaters placed at side surfaces of the assembly provided heating of the assembly. The difference between graphite temperature in different points of the assembly did not exceed 20°C and for the region of the measured cell 10°C.

Most of the measurements of neutron spectra were carried out at graphite temperatures of 523°K and 613°K with neutron energy resolution of 20 μsec/m. The results of neutron spectrum measurements at the slug centre and in graphite at the boundary of the cell and at graphite temperature 613°K are presented in Figs 12, 11. The calculated results from reference [23] are also shown in the figures. The satisfactory agreement between the calculated and measured spectra for graphite is to be noted. The calculations show negligible anisotropy of neutron spectra at the cell boundary. The corresponding vector flux spectra in the other directions coinside with the curves shown in the figures.

There is a considerable spectrum anisotropy in the slug (Fig.12). The neutron spectrum calculated in the direction parallel to the uranium slug axis coincide with the measured spectrum. The "neutron temperature" dependence throughout the cell is shown in Fig.13. The presented "temperatures" were calculated from average velocity, average inverse velocity and the most probable velocity U_m in the distribution $v^2 \cdot n(v)$ by using the formulae providing th relation between these values and the temperature for the Maxwell distribution. The difference in "temperature" absolute values is due to non-Maxwell shape of the neutron spectrum in the region of averaging (from 0.44 ev down to 0.0086 ev). Neutron spectrum in the moderator changes with the coordinate very little as well as in the case of the uranium-water lattice. For uranium the neutron spectrum was measured at the centre of the slug only, but it seemed to be likely that there was only a little change of this spectrum along the radius of the slug in case of the uranium-water lattice.Coats and Gayther (24) have also measured the neutron spectra in the uranium-water lattice. The lattice spacing used in their experiment was the same as that in our case. The diameter of the slug (2.95 cm) and the air gap around the slug were somewhat different. These authors presented the results of neutron spectrum measurements carried out at various graphite temperatures only in graphite in the middle between the slugs only.

367

III. Experimental Investigation on Process of Setting up of Equilibrium Neutron Energy Spectra

The effect of chemical bond is known to effect on the form of the stationary thermal neutron spectrum only in the case of presence of a rather intensive absorption. Nevertheless "poisoning" of the system by introducing the absorber is complicated in many cases and connected with a considerable lack of intensity of the measured neutron flux. Investigation of the time setting up of equilibrium spectrum in pure moderator makes possible to obtain the information about the role of chemical bond in the thermalization process. Such information is as so complete as that from stationary spectrum measurements. But the necessity of poisoning the system vanishes in this case. It should be noted also that these investigations give directly the values of some important parameters characterizing the process of time setting up of energy equilibrium spectrum. The time interval necessary for setting up of neutron energy equilibrium with the medium is just one of such parameters. The work by Bernard et al (25) is up to now the only reported one devoted to studying of the transitional neutron spectra.

1. Measurement Procedure

Scheme of ecperimental arrangement is presented at Fig.I4. The electron beam of the linear accelerator [26] was deflected with the help of a special magnetic system with a cross field and struck the lead target inside the investigated moderator producing short (1 μsec duration) bursts of fast neutrons with frequency I00 Hz. The neutron beam was extracted from the moderator, the spectrum measurments being carried out at different time intervals after fast neutron bursts by time-flight technique with the help of a mechanical chopper synchronized to the accelerator operation. There were two divergent slits in the chopper which provided the constancy of the transmission function within all range of neutron energies investigated at the minimum neutron pulse duration of 5 μsec. The detector consisting of 95 proportional BF_3-counters was placed at 4 meters from the shopper. The peculiarity of transitional spectrum measurements consisted in some additional distrosion of the spectrum due to neutron motion from the bottom of the cavity in the moderator into the mechanical chopper. This spectrum transformation had been also accounted for in the experimental data treatment.

2. Results of Measurements

Transitional spectra were investigated in graphite and beryllium prisms with dimensions of 60 cm x 60 cm x 45 cm at time intervals from 80 μsec to I500 μsec and from 50 μsec to 800 μsec for graphite and beryllium respectively. The neutron beam was taken from the centre of the prism through the cavity I0 cm x I0 cm. So the neutron spectrum measurements in different points of the beryllium prizm showed that gradient effect of the neutron flux was small and lay in within the limits of statistical errors of measurements.

The results of measurements of the transitional spectra in graphite and beryllium are given in Figs I5 and I6.

Consider some peculiarities of neutron spectra behaviour in the regions of small and large time of moderation. In small moderation time region when the neutron energy is still high the nuclei of moderator can be considered as freeones. Then one can calculated the neutron spectrum [27, 28]. The dependence of average neutron energy on the time of moderation $E = f(t)$ for beryllium and graphite calculated from the experimental spectra and from the results of reference (28) is presented on Fig.I7.

It can be easily noticed that ecperimental values of $\bar{E}$ lie considerably higher than calculated ones within the whole investigated range. This result testifies to crystal atomic bond in graphite and beryllium being manifesting at sufficiently high energies of neutrons ($\sim$ 0.2 eV). It should be pointed out that at small moderation time close to the time of duration of chopper neutron pulse a large uncertainty in moderation time value arises. This circumstance leads to overestimation of E.

When the time of moderation becomes considerable large the equilibrium velocity distribution of neutrons is to be achieved. From Fig.I5 and I6 one can see that in the region of small energies there is a deviation of experimental points from the Maxwell distribution. This deviation decreases as the t rises. For graphite, starting from $t \approx 640$ μsec and for beryllium with $t \approx 200$ μsec, the main part of the spectrum can be expressed by Maxwell distribution with $kT = 25.5$ MeV.

The average energy E slowly decreases at large time of moderation and aims at some asymptotic value. The investigated time range seems to be insufficient for the determination of average energy E of

equilibrium spectrum which should be set up in the system. At ~700 μsec in the case of beryllium and at ~1400 μsec for the graphite the acerage energy of the spectrum does not yet reach the value $E_{p\infty} = \frac{3}{2}$ kT which corresponds to the medium of the infinite sizes.

It is known that in the medium of finite size the value E_p must be less than $\frac{3}{2}$ kT because of the diffusion cooling. So more time is required for the setting up of the equilibrium energy distribution than that studied in our case. The rate of setting up of the thermal neutron equilibrium spectrum is described usually by the thermalization time According to elementary theory of thermalization average spectrum energy E approaches with time to the equilibrium value of the exponential law [29] :

$$E(t) - E_p \sim \exp\left(-\frac{t}{\tau_{th}}\right) \qquad (3)$$

However, it is difficult to represent the obtained experimental dependence E = f (t) by such a simple relation. Therefore the process of setting up of the equilibrium neutron spectrum can bot be described in terms of the only parameter sucn as a thermalization time τ_{th} The thermalization in different moderators can be described qualitatively by the time interval necessary for the setting up of the complete ewuilibrium. Our results of the experiments conducted show that this time corresponds to nearly 2000 μsec for graphite and nearly 1000 μsec for beryllium. It is interesting to note that the calculations based on the model of monoatomic heavy gas (30) give for the fiven times the values 230 μsec for graphite and 140 μsec for beryllium. These results testify to the strong effect of chemical bonds of moderator atoms on the rate of setting up of thermal equilibrium of neutrons with a medium.

Conclusion

The conducted experiments do not exhaust the planned program of the investigations. This program includes a detailed studying of a more number of moderators and multiplication systems in a wide range of temperature and neutron energies.

The investigations of neutron thermalization is continuing now. The construction of a new multidetector installation for measurements of double differential cross sections with high accuracy and resolution is being completed. The investigation of neutron thermalization in media at high temperature gradients is being carried out on. The problem

of spectrum anisotropy in heterogeneous media is expected to be studied in detail as well as the question of setting up of the equilibrium neutron spectrum in hydrogenous moderators, etc.

x x x

The sutdies of neutron thermalization at IAE were initiated by I.V.Kurchatov. Later these investigations were developed due to support and constant interest shown by Academician A.P.Aleksandrov.

References

I. И.В.Курчатов, "Некоторые вопросы развития атомной энергетики в СССР. Доклад в Харуэлле, 1956 г.

2. P.A.Egelstaff. Symposium on inelastic scattering of neutrons in solids and liquids. Vienna, 1960.

3. P.A.Egelstaff. Nucl.Science and Eng., 12 (1962) 250.

4. P.A. Egelstaff. P.Schofield. Nucl.Science and Eng., 12 (1962) 260

5. P.A. Egelstaff., B.C.Haywood and I.M.Thorson. Symposium on inelastic scattering of neutrons in solids and liquids. Chalk River, 1962.

6. K.E. Larsson, U.Dahlborg, Symposium on inelastic scattering of neutrons in solids and liquids, Chalk River, 1962.

7. Л.В Майоров, В.Ф.Турчин, М.С.Юдкевич "Влияние химической связи на термализацию нейтронов". Доклад на Ш Международной конференции по использованию атомной энергии в мирных целях. Женева, 1964 г.

8. В.И.Мостовой, В.С.Дикарев, М.Б.Егиазаров, Ю.С.Салтыков. Труды П Международной конференции по мирному использованию атомной энергии. Доклады советских ученых, П (1959), 546.

9. В.С.Дикарев, М.Б.Егиазаров, В.И.Мостовой. Ю.С.Салтыков. Доклад на конференции в Дрездене. 1960 г.

10. Г.И.Марчук, В.Ф.Турчин, В.В.Смелов, Г.А.Илясова. Атомная энергия 13, вып.6 (1962), 534.

11. Е.Я.Доильницын, А.Г.Новиков. Атомная энергия 13, вып.5 (1962), 491.

12. M.J.Poole.Jorn. of Nucl.Energy, Y (1957) 325

I3. R.B.Walton, J.R.Beyster, J.L.Wood, W.M.Lopez.Symposium on inelastic scattering of neutrons in solids and liquids, Vienna, I960.

I4. J.R.Beyster, J.L.Wood, W.M.Lopez, R.B.Walton.Nucl.Science and Eng., 9 (I96I) I68.

I5.K.Burkart , W.Reichardt.Proceedings of the Brookhaven conference on neutron thermalization, I962.

I6. R.S.Stone, R.E.Slovacek.Nucl.Science and Eng., 6(I959) 466

I7. R.R.Coveyou, R.R.Bates, B.K.J.Osborne.Jorn.of Nucl.Energy,II(I956)3.

I8. В.И.Мостовой, В.С.Дикарев, М.Б.Егиазаров, Ю.С.Салтыков Атомная энергия I3, вып. 6 (I962) 546.

I9. А.Н.Тихонов. Доклады Академии наук СССР, I49 (I963) 529.

20. L. de Sobrino, M.Clark. Nucl.Science and Eng.,IO (I96I) 377

2I. H.C.Honeck, H.Takahashi.BNL-5924 (I962)

22. Кэмпбелл К. и др. Труды П Международной конференции по мирному использованию атомной энергии. Избранные доклады иностранных ученых П (I959), 477.

23. Г.И.Марчук, Г.А.Илясова, В.И.Морозов, В.В. Смелов, В.А.Ходаков "Расчеты спектров медленных нейтронов". Доклад на Ш Международной конференции по использованию атомной энергии в мирных целях, Женева, I964.

24. M.S.Coates, D.B.Cayther. AERE-R3829 (I96I)

25. B.Barnard, N.A Khan,M.J.Poole,J.H.Tait, R.C.F.McLatchie. Proceedings of the Brookhaven conference on neutron thermalization I962.

26. Р.М.Воронков, М.П.Певзнер и др. Атомная энергия I3, вып.4 (I962) 327.

27 М.В.Казарновский. Атомная энергия 4, вып.6 (I958),539

28 И.Г.Дядькин, Э.П.Баталина. Атомная энергия I0, вып.I (I96I) 5

29. K.Wirtz, K.H.Beckurts. Elementare Neutronenphysik. Springer-Verlag. Berlin,I958.

30. S.N.Purohit.Nucl.Science and Eng.,9(I96I) 305

3I. Дроздов С.И., Зарецкий Д.Ф., Кудрин Л.П.,Сидельников Т.Х. Доклад на П Международной конференции по мирному использованию атомной энергии.Женева, I958.

32. M.D.Nelkin.Phys.Rev.,II9(I96I) 74

33. D.A.Kottwits,B.F.Leonard.Symposium on inelastic scattering of neutrons in solids and liquids, Chalk River, I962.

367

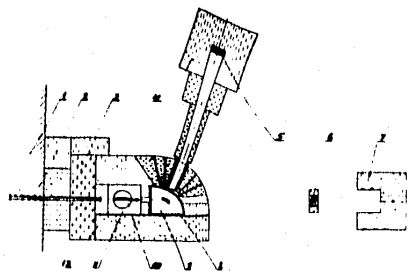

Fig.1. Scheme of experimental installation for double differential cross-section measurements
1 - shielding of the VVR-M reactor 2 -Experimental hole of the reactor 3 - Stationary shielding of the installation 4 - Mobile protection of scattered beam detector 5. Scattered beam detector (BF_3 - counter assembly) 6. Straight beam monitor 7. Beam trap 8. Scatterer 9. Chamber of scatterer 10. Mechanical monochromator 11. Chamber of monochromator 12. Mobile protection of monochromator and scatterer

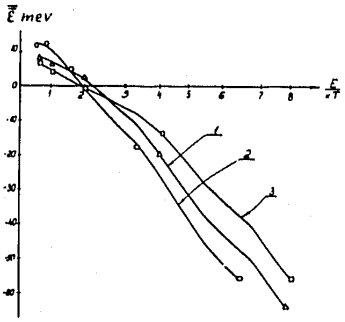

Fig.3a. The dependence of average energy variation with scattering on the energy of incident neutrons.
1 - H_2O; T = 23°C; 2 - H_2O; T=90°C; 3-$C_{15}H_{16}$; T = 17°C.

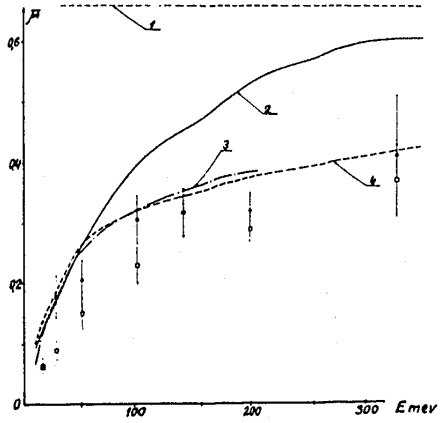

Fig.3b. The dependence of average cosine $\bar{\mu}$ of neutron scattering angle on the incident neutron energy E.
1 - (E) for resting nuclei with M=1;
2 - (E) for the gas with Meff = f(E) (31);
3 - (E) calculated in ref.(7);
4 - (E) calculated using Nelkin Model (32);
Points(•) show experimental values of $\bar{\mu}$ (E) for H_2O at temperature 296°K.
Squares(□) correspond to experimental values of $\bar{\mu}$ (E) for $C_{15}H_{16}$ at temperature 290°K.

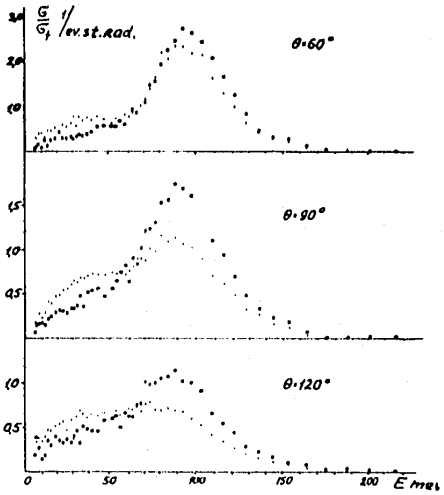

Fig.2 The ratio of double differential cross-section to free atom scattering cross section for H_2O and $C_{15}H_{16}$. E = 100 Mev.
x - H_2O(T=23°C), R=18%. ● -$C_{15}H_{16}$(T=17°C), R=18%.

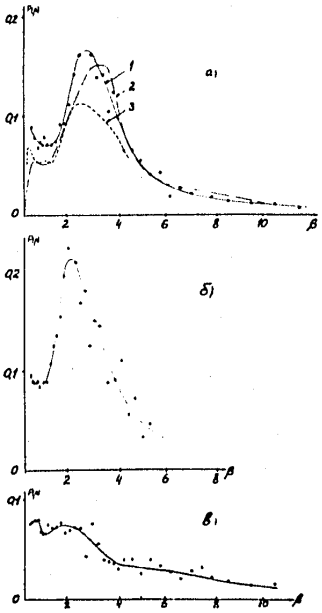

Fig.4. а) Spectra P(β) for H_2O at T=23°C
1 - result given in the paper
2 - measurements by Egelstaff, Haywood and Torson(5) and Kottwitz and Leonard (33);
3 - measurements by Larsson and Dallborg (6)
б) Spectrum P(β) for H_2O at T=90°C
в) Spectrum P(β) for $C_{15}H_{16}$ at T=17°C

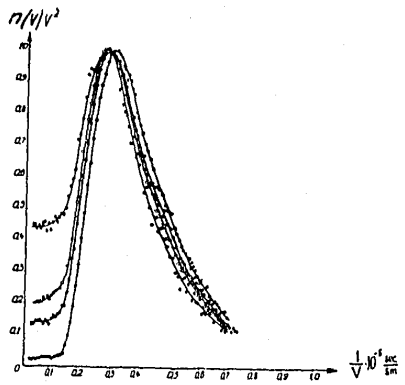

Fig.5 Neutron spectra in pure water and in water poisoned with boron
● - absorption 4.83 $\frac{\text{barn}}{\text{H atom}}$; ○ - absorption 2.25 $\frac{\text{barn}}{\text{atom H}}$;
⊙ - absorption 1.50 $\frac{\text{barn}}{\text{atom H}}$; ◐ - absorption 0.33 $\frac{\text{barn}}{\text{atom H}}$.

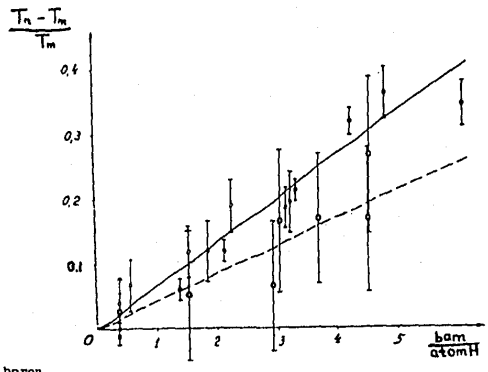

Fig.6. The dependence of neutron temperature excess above the medium temperature on the absorber concentration
○ - results presented in this paper; ◐ - results given in reference (12)
◒ - results given in reference (15) ⊙ - results given in reference (11)
● - results given in reference (14)

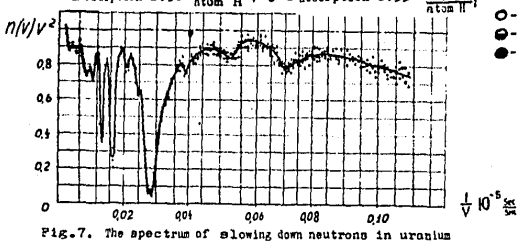

Fig.7. The spectrum of slowing down neutrons in uranium of the uranium-water lattice with spacing 5.5 cm.

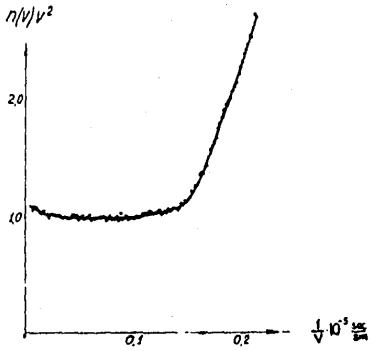

Fig.8. The spectrum of slowing down neutrons in the water of the uranium-water lattice with spacing 5.5 cm.

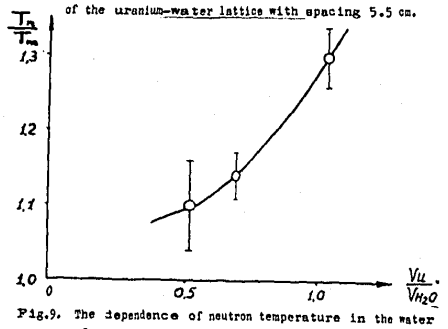

Fig.9. The dependence of neutron temperature in the water of uranium-water lattices on uranium concentration.

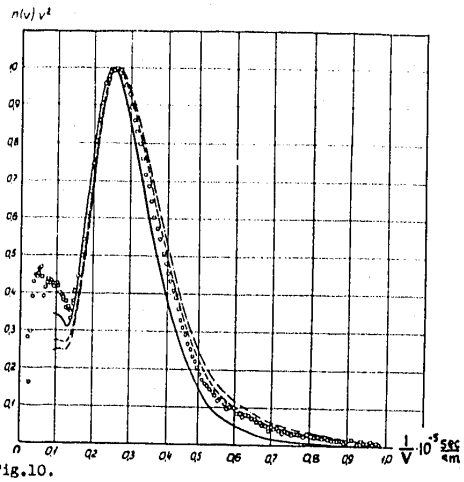

Fig.10.

Neutron spectrum in uranium of the uranium-water lattice with spacing 5.5 cm; temperature of the water is 323°K.

Solid line (-) shows the neutron spectrum in the direction of slug axis. Dashed-pointed curve (-·-·-) represents neutron spectrum in the perpendicular direction to slug axis. Dashed curve (---) corresponds to scalar flux.

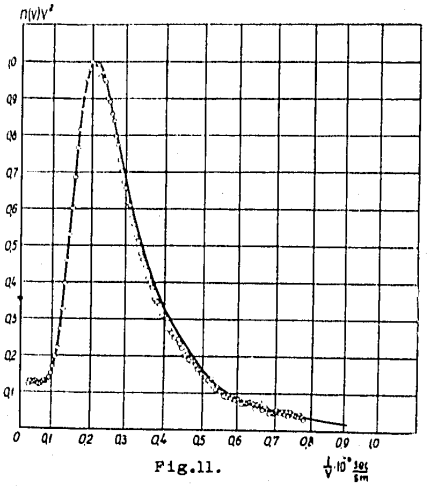

Fig.11.

Neutron spectrum in graphite at the cell boundary of uranium-graphite lattice; graphite temperature is 613°K. Circles (o) show experimental data. Solid line (-) demonstrates the calculation.

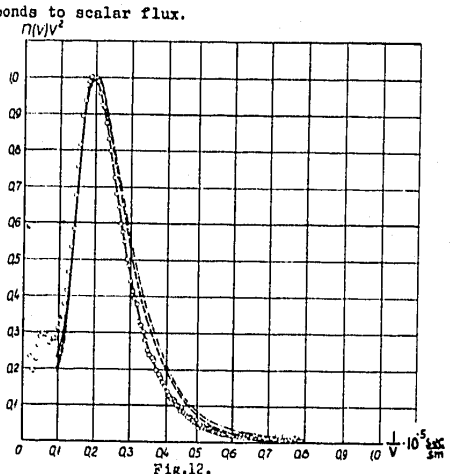

Fig.12.

Neutron spectrum in uranium of uranium-graphite lattice. Graphite temperature is 613°K.

Solid line (-) shows the neutron spectrum in the direction of slug axis.

Dashed-pointed curve (-·-·-) represents neutron spectrum in the perpendicular direction to slug axis. Dashed curve (---) corresponds to scalar flux.

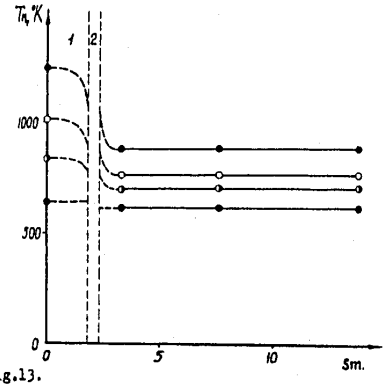

rig.13.

The "temperature" distribution of neutron gas throughout the cell of uranium-graphite lattice.

1 - fuel slug
2 - air and aluminium
› - graphite.

o - $T_n = \frac{\Sigma}{4} \cdot \frac{m(\bar{v})^2}{2\kappa}$; ⊙ - $T_n = \frac{4}{\pi} \cdot \frac{m}{2\kappa} \cdot \frac{1}{\left(\frac{1}{\bar{v}}\right)^2}$

o - $T_n = \frac{m v_m^2}{4\kappa}$; ● - medium temperature.

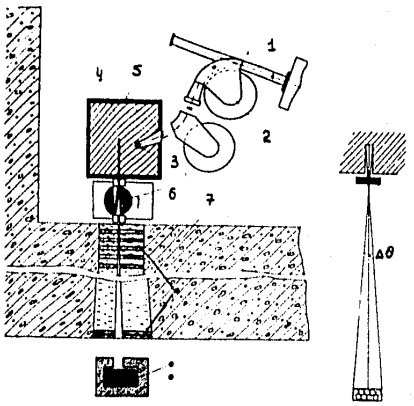

Fig.14. The scheme of experimental installation for studying the process of neutron thermalization.

1 - Vacuum tube of linear accelerator
2 - Deflecting and focusing magnets
3 - Lead target
4 - Prism of material investigated
5 - Prism protection (B_4C)
6 - Chopper
7 - Biological shielding of the accelerator bunker
8 - Lead diaphragms
9 - Detector
10 - Detector shielding

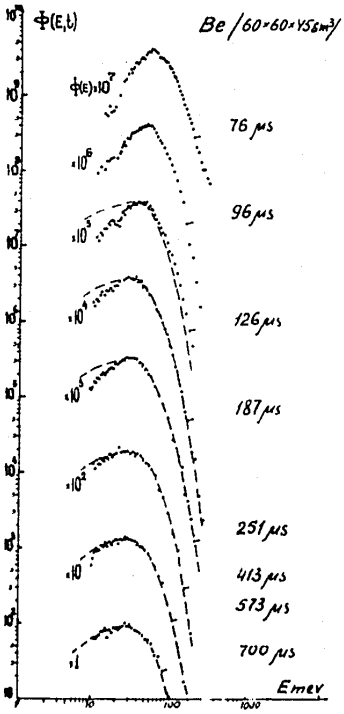

Fig.16. Neutron flux $\phi(E,t)$ in beryllium.
---Maxwell spectrum T = 300°K.

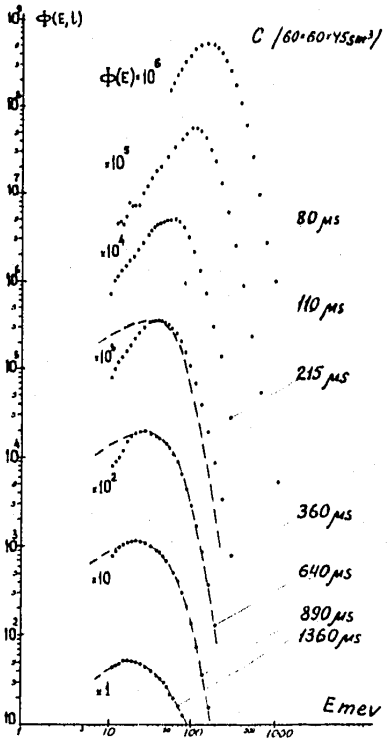

Fig.15. Neutron flux $\phi(E,t)$ in graphite.
--- Maxwell spectrum T=300°K.

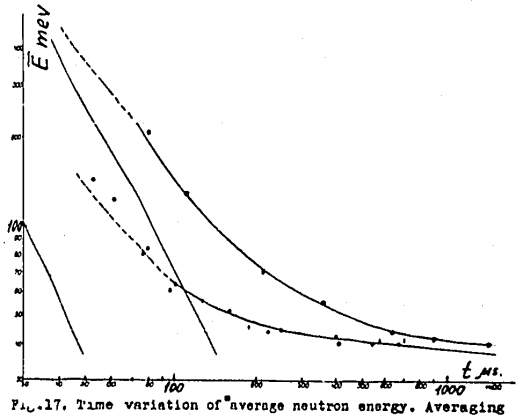

Fig.17. Time variation of average neutron energy. Averaging is carried out over the neutron density. Relations $\bar{E} = f(t)$ calculated for graphite and beryllium using the model of free resting nuclei (28) are presented by sloping straight lines.

⊖ - Experimental values $\bar{E}$ for graphite (centre of prism)
⊖● - Experimental values $\bar{E}$ for beryllium at a distance of 10 cm (⊖) and 20 cm (●) from the centre of prism.

367

Table I The Scattering Law for H_2O (T = 23°C)

β	$S(\alpha,\beta)\cdot 10^3$
0.0	0.004 0.004 0.007 0.009 0.007 0.005 4.000 3.02 2.87 2.66 2.03 1.44
0.1	0.002 0.003 0.005 0.004 0.003 0.002 0.002 0.002 0.002 0.002 0.002 0.002 0.002 0.002 0.002 0.002 0.002 0.002 0.002 0.002 2.56 2.37 2.14 1.94 1.76 1.60 1.46 1.33 1.22 1.13 1.04 0.97 0.90 0.84 0.79 0.74 0.70 0.66
0.2	0.010 0.014 0.014 0.013 0.012 0.010 0.009 0.008 0.008 0.007 0.007 0.006 0.006 0.006 0.005 0.005 0.005 0.005 1.94 1.79 1.65 1.53 1.42 1.32 1.23 1.15 1.08 1.01 0.95 0.89 0.84 0.79 0.75 0.71 0.67 0.64
0.3	0.017 0.020 0.021 0.020 0.019 0.017 0.016 0.015 0.014 0.013 0.012 0.011 0.011 0.010 0.010 0.009 0.009 0.008 1.57 1.46 1.36 1.27 1.19 1.11 1.04 0.98 0.92 0.87 0.82 0.78 0.74 0.70 0.67 0.64 0.61 0.58
0.4	0.024 0.027 0.028 0.028 0.027 0.026 0.025 0.024 0.023 0.022 0.021 0.020 0.019 0.018 0.017 0.016 0.016 0.015 1.31 1.23 1.15 1.08 1.02 0.96 0.91 0.86 0.81 0.77 0.73 0.69 0.66 0.63 0.60 0.57 0.55 0.52
0.5	0.031 0.034 0.035 0.035 0.034 0.033 0.032 0.031 0.030 0.029 0.028 0.027 0.026 0.025 0.024 0.023 0.022 0.021 1.12 1.06 1.00 0.94 0.89 0.84 0.80 0.76 0.72 0.69 0.66 0.63 0.60 0.57 0.55 0.53 0.51 0.49
0.6	0.038 0.041 0.042 0.042 0.041 0.040 0.039 0.038 0.037 0.036 0.035 0.034 0.033 0.032 0.031 0.030 0.029 0.028 0.98 0.93 0.88 0.84 0.80 0.76 0.73 0.70 0.67 0.64 0.62 0.59 0.57 0.55 0.53 0.51 0.49 0.48
0.7	0.045 0.048 0.049 0.049 0.048 0.047 0.046 0.045 0.044 0.043 0.042 0.041 0.040 0.039 0.038 0.037 0.036 0.035 0.87 0.83 0.79 0.76 0.73 0.70 0.67 0.65 0.63 0.61 0.59 0.57 0.55 0.53 0.52 0.50 0.49 0.47
0.8	0.052 0.055 0.056 0.056 0.055 0.054 0.053 0.052 0.051 0.050 0.049 0.048 0.047 0.046 0.045 0.044 0.043 0.042 0.78 0.74 0.71 0.68 0.66 0.63 0.61 0.59 0.57 0.55 0.53 0.52 0.50 0.49 0.48 0.46 0.45 0.44
0.9	0.059 0.062 0.063 0.063 0.062 0.061 0.060 0.059 0.058 0.057 0.056 0.055 0.054 0.053 0.052 0.051 0.050 0.049 0.70 0.67 0.64 0.62 0.60 0.57 0.56 0.54 0.52 0.50 0.49 0.47 0.46 0.45 0.44 0.43 0.42 0.41
1.0	0.066 0.069 0.070 0.070 0.069 0.068 0.067 0.066 0.065 0.064 0.063 0.062 0.061 0.060 0.059 0.058 0.057 0.056 0.63 0.60 0.58 0.56 0.54 0.52 0.50 0.48 0.47 0.45 0.44 0.43 0.41 0.40 0.39 0.38 0.37 0.36
1.1	0.073 0.076 0.077 0.077 0.076 0.075 0.074 0.073 0.072 0.071 0.070 0.069 0.068 0.067 0.066 0.065 0.064 0.063 0.57 0.54 0.52 0.50 0.49 0.47 0.45 0.44 0.42 0.41 0.40 0.39 0.38 0.37 0.36 0.35 0.34 0.33
1.2	0.080 0.083 0.084 0.084 0.083 0.082 0.081 0.080 0.079 0.078 0.077 0.076 0.075 0.074 0.073 0.072 0.071 0.070 0.52 0.49 0.47 0.46 0.44 0.43 0.41 0.40 0.38 0.37 0.36 0.35 0.34 0.33 0.32 0.31 0.30 0.30
1.3	0.087 0.090 0.091 0.091 0.090 0.089 0.088 0.087 0.086 0.085 0.084 0.083 0.082 0.081 0.080 0.079 0.078 0.077 0.47 0.45 0.43 0.41 0.40 0.38 0.37 0.36 0.34 0.33 0.32 0.31 0.31 0.30 0.29 0.28 0.27 0.27
1.4	0.094 0.097 0.098 0.098 0.097 0.096 0.095 0.094 0.093 0.092 0.091 0.090 0.089 0.088 0.087 0.086 0.085 0.084 0.43 0.41 0.39 0.38 0.36 0.35 0.33 0.32 0.31 0.30 0.29 0.28 0.27 0.27 0.26 0.25 0.25 0.24
1.5	0.101 0.104 0.105 0.105 0.104 0.103 0.102 0.101 0.100 0.099 0.098 0.097 0.096 0.095 0.094 0.093 0.092 0.091 0.39 0.37 0.35 0.34 0.33 0.31 0.30 0.29 0.28 0.27 0.26 0.25 0.24 0.24 0.23 0.22 0.22 0.21
1.6	0.108 0.111 0.112 0.112 0.111 0.110 0.109 0.108 0.107 0.106 0.105 0.104 0.103 0.102 0.101 0.100 0.099 0.098 0.35 0.33 0.32 0.30 0.29 0.28 0.27 0.26 0.25 0.24 0.23 0.22 0.22 0.21 0.20 0.20 0.19 0.19
1.7	0.115 0.118 0.119 0.119 0.118 0.117 0.116 0.115 0.114 0.113 0.112 0.111 0.110 0.109 0.108 0.107 0.106 0.105 0.32 0.30 0.29 0.27 0.26 0.25 0.24 0.23 0.22 0.21 0.21 0.20 0.19 0.19 0.18 0.17 0.17 0.16
1.8	0.122 0.125 0.126 0.126 0.125 0.124 0.123 0.122 0.121 0.120 0.119 0.118 0.117 0.116 0.115 0.114 0.113 0.112 0.29 0.27 0.26 0.25 0.24 0.23 0.22 0.21 0.20 0.19 0.19 0.18 0.17 0.17 0.16 0.16 0.15 0.15
1.9	0.129 0.132 0.133 0.133 0.132 0.131 0.130 0.129 0.128 0.127 0.126 0.125 0.124 0.123 0.122 0.121 0.120 0.119 0.26 0.25 0.24 0.23 0.22 0.21 0.20 0.19 0.18 0.18 0.17 0.16 0.16 0.15 0.15 0.14 0.14 0.13
2.0	0.136 0.139 0.140 0.140 0.139 0.138 0.137 0.136 0.135 0.134 0.133 0.132 0.131 0.130 0.129 0.128 0.127 0.126 0.24 0.23 0.22 0.21 0.20 0.19 0.18 0.18 0.17 0.16 0.16 0.15 0.14 0.14 0.13 0.13 0.12 0.12
2.1	0.143 0.146 0.147 0.147 0.146 0.145 0.144 0.143 0.142 0.141 0.140 0.139 0.138 0.137 0.136 0.135 0.134 0.133 0.22 0.21 0.20 0.19 0.18 0.17 0.17 0.16 0.15 0.15 0.14 0.14 0.13 0.13 0.12 0.12 0.11 0.11
2.2	0.150 0.153 0.154 0.154 0.153 0.152 0.151 0.150 0.149 0.148 0.147 0.146 0.145 0.144 0.143 0.142 0.141 0.140 0.20 0.19 0.18 0.17 0.17 0.16 0.15 0.15 0.14 0.13 0.13 0.12 0.12 0.11 0.11 0.10 0.10 0.09
2.3	0.157 0.160 0.161 0.161 0.160 0.159 0.158 0.157 0.156 0.155 0.154 0.153 0.152 0.151 0.150 0.149 0.148 0.147 0.18 0.17 0.16 0.16 0.15 0.14 0.14 0.13 0.12 0.12 0.11 0.11 0.10 0.10 0.09 0.09 0.08 0.08
2.4	0.164 0.167 0.168 0.168 0.167 0.166 0.165 0.164 0.163 0.162 0.161 0.160 0.159 0.158 0.157 0.156 0.155 0.154 0.17 0.16 0.15 0.14 0.14 0.13 0.13 0.12 0.11 0.11 0.10 0.10 0.09 0.09 0.08 0.08 0.07 0.07
2.5	0.171 0.174 0.175 0.175 0.174 0.173 0.172 0.171 0.170 0.169 0.168 0.167 0.166 0.165 0.164 0.163 0.162 0.161 0.15 0.14 0.14 0.13 0.12 0.12 0.11 0.11 0.10 0.09 0.09 0.08 0.08 0.08 0.07 0.07 0.06 0.06
2.6	0.178 0.181 0.182 0.182 0.181 0.180 0.179 0.178 0.177 0.176 0.175 0.174 0.173 0.172 0.171 0.170 0.169 0.168 0.14 0.13 0.13 0.12 0.11 0.11 0.10 0.10 0.09 0.09 0.08 0.08 0.07 0.07 0.07 0.06 0.06 0.05
2.7	0.185 0.188 0.189 0.189 0.188 0.187 0.186 0.185 0.184 0.183 0.182 0.181 0.180 0.179 0.178 0.177 0.176 0.175 0.13 0.12 0.12 0.11 0.10 0.10 0.09 0.09 0.08 0.08 0.07 0.07 0.07 0.06 0.06 0.06 0.05 0.05
2.8	0.192 0.195 0.196 0.196 0.195 0.194 0.193 0.192 0.191 0.190 0.189 0.188 0.187 0.186 0.185 0.184 0.183 0.182 0.12 0.11 0.11 0.10 0.10 0.09 0.09 0.08 0.08 0.07 0.07 0.06 0.06 0.06 0.05 0.05 0.05 0.04
2.9	0.199 0.202 0.203 0.203 0.202 0.201 0.200 0.199 0.198 0.197 0.196 0.195 0.194 0.193 0.192 0.191 0.190 0.189 0.11 0.10 0.10 0.09 0.09 0.08 0.08 0.07 0.07 0.06 0.06 0.06 0.05 0.05 0.05 0.04 0.04 0.04
3.0	0.206 0.209 0.210 0.210 0.209 0.208 0.207 0.206 0.205 0.204 0.203 0.202 0.201 0.200 0.199 0.198 0.197 0.196 0.10 0.09 0.09 0.08 0.08 0.07 0.07 0.06 0.06 0.06 0.05 0.05 0.05 0.04 0.04 0.04 0.03 0.03
3.1	0.213 0.216 0.217 0.217 0.216 0.215 0.214 0.213 0.212 0.211 0.210 0.209 0.208 0.207 0.206 0.205 0.204 0.203 0.09 0.08 0.08 0.07 0.07 0.06 0.06 0.06 0.05 0.05 0.05 0.04 0.04 0.04 0.03 0.03 0.03 0.03
3.2	0.220 0.223 0.224 0.224 0.223 0.222 0.221 0.220 0.219 0.218 0.217 0.216 0.215 0.214 0.213 0.212 0.211 0.210 0.08 0.08 0.07 0.07 0.06 0.06 0.06 0.05 0.05 0.05 0.04 0.04 0.04 0.03 0.03 0.03 0.03 0.02
3.3	0.227 0.230 0.231 0.231 0.230 0.229 0.228 0.227 0.226 0.225 0.224 0.223 0.222 0.221 0.220 0.219 0.218 0.217 0.07 0.07 0.06 0.06 0.06 0.05 0.05 0.05 0.04 0.04 0.04 0.03 0.03 0.03 0.03 0.02 0.02 0.02
3.4	0.234 0.237 0.238 0.238 0.237 0.236 0.235 0.234 0.233 0.232 0.231 0.230 0.229 0.228 0.227 0.226 0.225 0.224 0.06 0.06 0.06 0.05 0.05 0.05 0.04 0.04 0.04 0.03 0.03 0.03 0.03 0.02 0.02 0.02 0.02 0.02
3.5	0.241 0.244 0.245 0.245 0.244 0.243 0.242 0.241 0.240 0.239 0.238 0.237 0.236 0.235 0.234 0.233 0.232 0.231 0.06 0.05 0.05 0.05 0.04 0.04 0.04 0.04 0.03 0.03 0.03 0.03 0.02 0.02 0.02 0.02 0.02 0.02
3.6	0.248 0.251 0.252 0.252 0.251 0.250 0.249 0.248 0.247 0.246 0.245 0.244 0.243 0.242 0.241 0.240 0.239 0.238 0.05 0.05 0.05 0.04 0.04 0.04 0.04 0.03 0.03 0.03 0.03 0.02 0.02 0.02 0.02 0.02 0.02 0.02
3.7	0.255 0.258 0.259 0.259 0.258 0.257 0.256 0.255 0.254 0.253 0.252 0.251 0.250 0.249 0.248 0.247 0.246 0.245 0.05 0.04 0.04 0.04 0.04 0.03 0.03 0.03 0.03 0.03 0.02 0.02 0.02 0.02 0.02 0.02 0.02 0.02
3.8	0.262 0.265 0.266 0.266 0.265 0.264 0.263 0.262 0.261 0.260 0.259 0.258 0.257 0.256 0.255 0.254 0.253 0.252 0.04 0.04 0.04 0.04 0.03 0.03 0.03 0.03 0.02 0.02 0.02 0.02 0.02 0.02 0.02 0.02 0.02 0.02
3.9	0.269 0.272 0.273 0.273 0.272 0.271 0.270 0.269 0.268 0.267 0.266 0.265 0.264 0.263 0.262 0.261 0.260 0.259 0.04 0.04 0.03 0.03 0.03 0.03 0.03 0.02 0.02 0.02 0.02 0.02 0.02 0.02 0.02 0.02 0.02 0.02
4.0	0.276 0.279 0.280 0.280 0.279 0.278 0.277 0.276 0.275 0.274 0.273 0.272 0.271 0.270 0.269 0.268 0.267 0.266 0.03 0.03 0.03 0.03 0.03 0.02 0.02 0.02 0.02 0.02 0.02 0.02 0.02 0.02 0.02 0.02 0.02 0.02
4.1	0.283 0.286 0.287 0.287 0.286 0.285 0.284 0.283 0.282 0.281 0.280 0.279 0.278 0.277 0.276 0.275 0.274 0.273 0.03 0.03 0.03 0.03 0.02 0.02 0.02 0.02 0.02 0.02 0.02 0.02 0.02 0.02 0.02 0.02 0.02 0.02
4.2	0.290 0.293 0.294 0.294 0.293 0.292 0.291 0.290 0.289 0.288 0.287 0.286 0.285 0.284 0.283 0.282 0.281 0.280 0.03 0.03 0.03 0.02 0.02 0.02 0.02 0.02 0.02 0.02 0.02 0.02 0.02 0.02 0.02 0.02 0.02 0.02
4.3	0.297 0.300 0.301 0.301 0.300 0.299 0.298 0.297 0.296 0.295 0.294 0.293 0.292 0.291 0.290 0.289 0.288 0.287 0.02 0.02 0.02 0.02 0.02 0.02 0.02 0.02 0.02 0.02 0.02 0.02 0.02 0.02 0.02 0.02 0.02 0.02
4.4	0.304 0.307 0.308 0.308 0.307 0.306 0.305 0.304 0.303 0.302 0.301 0.300 0.299 0.298 0.297 0.296 0.295 0.294 0.02 0.02 0.02 0.02 0.02 0.02 0.02 0.02 0.02 0.02 0.02 0.02 0.02 0.02 0.02 0.02 0.02 0.02
4.5	0.311 0.314 0.315 0.315 0.314 0.313 0.312 0.311 0.310 0.309 0.308 0.307 0.306 0.305 0.304 0.303 0.302 0.301 0.02 0.02 0.02 0.02 0.02 0.02 0.02 0.02 0.02 0.02 0.02 0.02 0.02 0.02 0.02 0.02 0.02 0.02
4.6	0.318 0.321 0.322 0.322 0.321 0.320 0.319 0.318 0.317 0.316 0.315 0.314 0.313 0.312 0.311 0.310 0.309 0.308 0.02 0.02 0.02 0.02 0.02 0.02 0.02 0.02 0.02 0.02 0.02 0.02 0.02 0.02 0.02 0.02 0.02 0.02
4.7	0.325 0.328 0.329 0.329 0.328 0.327 0.326 0.325 0.324 0.323 0.322 0.321 0.320 0.319 0.318 0.317 0.316 0.315 0.02 0.02 0.02 0.02 0.02 0.02 0.02 0.02 0.02 0.02 0.02 0.02 0.02 0.02 0.02 0.02 0.02 0.02
4.8	0.332 0.335 0.336 0.336 0.335 0.334 0.333 0.332 0.331 0.330 0.329 0.328 0.327 0.326 0.325 0.324 0.323 0.322 0.02 0.02 0.02 0.02 0.02 0.02 0.02 0.02 0.02 0.02 0.02 0.02 0.02 0.02 0.02 0.02 0.02 0.02
4.9	0.339 0.342 0.343 0.343 0.342 0.341 0.340 0.339 0.338 0.337 0.336 0.335 0.334 0.333 0.332 0.331 0.330 0.329 0.02 0.02 0.02 0.02 0.02 0.02 0.02 0.02 0.02 0.02 0.02 0.02 0.02 0.02 0.02 0.02 0.02 0.02
5.0	0.346 0.349 0.350 0.350 0.349 0.348 0.347 0.346 0.345 0.344 0.343 0.342 0.341 0.340 0.339 0.338 0.337 0.336 0.02 0.02 0.02 0.02 0.02 0.02 0.02 0.02 0.02 0.02 0.02 0.02 0.02 0.02 0.02 0.02 0.02 0.02
5.1	0.353 0.356 0.357 0.357 0.356 0.355 0.354 0.353 0.352 0.351 0.350 0.349 0.348 0.347 0.346 0.345 0.344 0.343 0.02 0.02 0.02 0.02 0.02 0.02 0.02 0.02 0.02 0.02 0.02 0.02 0.02 0.02 0.02 0.02 0.02 0.02
5.2	0.360 0.363 0.364 0.364 0.363 0.362 0.361 0.360 0.359 0.358 0.357 0.356 0.355 0.354 0.353 0.352 0.351 0.350 0.02 0.02 0.02 0.02 0.02 0.02 0.02 0.02 0.02 0.02 0.02 0.02 0.02 0.02 0.02 0.02 0.02 0.02
5.3	0.367 0.370 0.371 0.371 0.370 0.369 0.368 0.367 0.366 0.365 0.364 0.363 0.362 0.361 0.360 0.359 0.358 0.357 0.02 0.02 0.02 0.02 0.02 0.02 0.02 0.02 0.02 0.02 0.02 0.02 0.02 0.02 0.02 0.02 0.02 0.02
5.4	0.374 0.377 0.378 0.378 0.377 0.376 0.375 0.374 0.373 0.372 0.371 0.370 0.369 0.368 0.367 0.366 0.365 0.364 0.02 0.02 0.02 0.02 0.02 0.02 0.02 0.02 0.02 0.02 0.02 0.02 0.02 0.02 0.02 0.02 0.02 0.02
5.5	0.381 0.384 0.385 0.385 0.384 0.383 0.382 0.381 0.380 0.379 0.378 0.377 0.376 0.375 0.374 0.373 0.372 0.371 0.02 0.02 0.02 0.02 0.02 0.02 0.02 0.02 0.02 0.02 0.02 0.02 0.02 0.02 0.02 0.02 0.02 0.02
5.6	0.388 0.391 0.392 0.392 0.391 0.390 0.389 0.388 0.387 0.386 0.385 0.384 0.383 0.382 0.381 0.380 0.379 0.378 0.02 0.02 0.02 0.02 0.02 0.02 0.02 0.02 0.02 0.02 0.02 0.02 0.02 0.02 0.02 0.02 0.02 0.02
5.7	0.395 0.398 0.399 0.399 0.398 0.397 0.396 0.395 0.394 0.393 0.392 0.391 0.390 0.389 0.388 0.387 0.386 0.385 0.02 0.02 0.02 0.02 0.02 0.02 0.02 0.02 0.02 0.02 0.02 0.02 0.02 0.02 0.02 0.02 0.02 0.02
5.8	0.402 0.405 0.406 0.406 0.405 0.404 0.403 0.402 0.401 0.400 0.399 0.398 0.397 0.396 0.395 0.394 0.393 0.392 0.02 0.02 0.02 0.02 0.02 0.02 0.02 0.02 0.02 0.02 0.02 0.02 0.02 0.02 0.02 0.02 0.02 0.02
5.9	0.409 0.412 0.413 0.413 0.412 0.411 0.410 0.409 0.408 0.407 0.406 0.405 0.404 0.403 0.402 0.401 0.400 0.399 0.02 0.02 0.02 0.02 0.02 0.02 0.02 0.02 0.02 0.02 0.02 0.02 0.02 0.02 0.02 0.02 0.02 0.02
6.0	0.416 0.419 0.420 0.420 0.419 0.418 0.417 0.416 0.415 0.414 0.413 0.412 0.411 0.410 0.409 0.408 0.407 0.406 0.02 0.02 0.02 0.02 0.02 0.02 0.02 0.02 0.02 0.02 0.02 0.02 0.02 0.02 0.02 0.02 0.02 0.02
6.1	0.423 0.426 0.427 0.427 0.426 0.425 0.424 0.423 0.422 0.421 0.420 0.419 0.418 0.417 0.416 0.415 0.414 0.413 0.02 0.02 0.02 0.02 0.02 0.02 0.02 0.02 0.02 0.02 0.02 0.02 0.02 0.02 0.02 0.02 0.02 0.02
6.2	0.430 0.433 0.434 0.434 0.433 0.432 0.431 0.430 0.429 0.428 0.427 0.426 0.425 0.424 0.423 0.422 0.421 0.420 0.02 0.02 0.02 0.02 0.02 0.02 0.02 0.02 0.02 0.02 0.02 0.02 0.02 0.02 0.02 0.02 0.02 0.02
6.3	0.437 0.440 0.441 0.441 0.440 0.439 0.438 0.437 0.436 0.435 0.434 0.433 0.432 0.431 0.430 0.429 0.428 0.427 0.02 0.02 0.02 0.02 0.02 0.02 0.02 0.02 0.02 0.02 0.02 0.02 0.02 0.02 0.02 0.02 0.02 0.02
6.4	0.444 0.447 0.448 0.448 0.447 0.446 0.445 0.444 0.443 0.442 0.441 0.440 0.439 0.438 0.437 0.436 0.435 0.434 0.02 0.02 0.02 0.02 0.02 0.02 0.02 0.02 0.02 0.02 0.02 0.02 0.02 0.02 0.02 0.02 0.02 0.02
6.5	0.451 0.454 0.455 0.455 0.454 0.453 0.452 0.451 0.450 0.449 0.448 0.447 0.446 0.445 0.444 0.443 0.442 0.441 0.02 0.02 0.02 0.02 0.02 0.02 0.02 0.02 0.02 0.02 0.02 0.02 0.02 0.02 0.02 0.02 0.02 0.02
6.6	0.458 0.461 0.462 0.462 0.461 0.460 0.459 0.458 0.457 0.456 0.455 0.454 0.453 0.452 0.451 0.450 0.449 0.448 0.02 0.02 0.02 0.02 0.02 0.02 0.02 0.02 0.02 0.02 0.02 0.02 0.02 0.02 0.02 0.02 0.02 0.02
6.7	0.465 0.468 0.469 0.469 0.468 0.467 0.466 0.465 0.464 0.463 0.462 0.461 0.460 0.459 0.458 0.457 0.456 0.455 0.02 0.02 0.02 0.02 0.02 0.02 0.02 0.02 0.02 0.02 0.02 0.02 0.02 0.02 0.02 0.02 0.02 0.02
6.8	0.472 0.475 0.476 0.476 0.475 0.474 0.473 0.472 0.471 0.470 0.469 0.468 0.467 0.466 0.465 0.464 0.463 0.462 0.02 0.02 0.02 0.02 0.02 0.02 0.02 0.02 0.02 0.02 0.02 0.02 0.02 0.02 0.02 0.02 0.02 0.02
6.9	0.479 0.482 0.483 0.483 0.482 0.481 0.480 0.479 0.478 0.477 0.476 0.475 0.474 0.473 0.472 0.471 0.470 0.469 0.02 0.02 0.02 0.02 0.02 0.02 0.02 0.02 0.02 0.02 0.02 0.02 0.02 0.02 0.02 0.02 0.02 0.02
7.0	0.486 0.489 0.490 0.490 0.489 0.488 0.487 0.486 0.485 0.484 0.483 0.482 0.481 0.480 0.479 0.478 0.477 0.476 0.02 0.02 0.02 0.02 0.02 0.02 0.02 0.02 0.02 0.02 0.02 0.02 0.02 0.02 0.02 0.02 0.02 0.02
7.1	0.493 0.496 0.497 0.497 0.496 0.495 0.494 0.493 0.492 0.491 0.490 0.489 0.488 0.487 0.486 0.485 0.484 0.483 0.02 0.02 0.02 0.02 0.02 0.02 0.02 0.02 0.02 0.02 0.02 0.02 0.02 0.02 0.02 0.02 0.02 0.02
7.2	0.500 0.503 0.504 0.504 0.503 0.502 0.501 0.500 0.499 0.498 0.497 0.496 0.495 0.494 0.493 0.492 0.491 0.490 0.02 0.02 0.02 0.02 0.02 0.02 0.02 0.02 0.02 0.02 0.02 0.02 0.02 0.02 0.02 0.02 0.02 0.02
7.3	0.507 0.510 0.511 0.511 0.510 0.509 0.508 0.507 0.506 0.505 0.504 0.503 0.502 0.501 0.500 0.499 0.498 0.497 0.02 0.02 0.02 0.02 0.02 0.02 0.02 0.02 0.02 0.02 0.02 0.02 0.02 0.02 0.02 0.02 0.02 0.02
7.4	0.514 0.517 0.518 0.518 0.517 0.516 0.515 0.514 0.513 0.512 0.511 0.510 0.509 0.508 0.507 0.506 0.505 0.504 0.02 0.02 0.02 0.02 0.02 0.02 0.02 0.02 0.02 0.02 0.02 0.02 0.02 0.02 0.02 0.02 0.02 0.02
7.5	0.521 0.524 0.525 0.525 0.524 0.523 0.522 0.521 0.520 0.519 0.518 0.517 0.516 0.515 0.514 0.513 0.512 0.511 0.02 0.02 0.02 0.02 0.02 0.02 0.02 0.02 0.02 0.02 0.02 0.02 0.02 0.02 0.02 0.02 0.02 0.02
7.6	0.528 0.531 0.532 0.532 0.531 0.530 0.529 0.528 0.527 0.526 0.525 0.524 0.523 0.522 0.521 0.520 0.519 0.518 0.02 0.02 0.02 0.02 0.02 0.02 0.02 0.02 0.02 0.02 0.02 0.02 0.02 0.02 0.02 0.02 0.02 0.02
7.7	0.535 0.538 0.539 0.539 0.538 0.537 0.536 0.535 0.534 0.533 0.532 0.531 0.530 0.529 0.528 0.527 0.526 0.525 0.02 0.02 0.02 0.02 0.02 0.02 0.02 0.02 0.02 0.02 0.02 0.02 0.02 0.02 0.02 0.02 0.02 0.02
7.8	0.542 0.545 0.546 0.546 0.545 0.544 0.543 0.542 0.541 0.540 0.539 0.538 0.537 0.536 0.535 0.534 0.533 0.532 0.02 0.02 0.02 0.02 0.02 0.02 0.02 0.02 0.02 0.02 0.02 0.02 0.02 0.02 0.02 0.02 0.02 0.02
7.9	0.549 0.552 0.553 0.553 0.552 0.551 0.550 0.549 0.548 0.547 0.546 0.545 0.544 0.543 0.542 0.541 0.540 0.539 0.02 0.02 0.02 0.02 0.02 0.02 0.02 0.02 0.02 0.02 0.02 0.02 0.02 0.02 0.02 0.02 0.02 0.02
8.0	0.556 0.559 0.560 0.560 0.559 0.558 0.557 0.556 0.555 0.554 0.553 0.552 0.551 0.550 0.549 0.548 0.547 0.546 0.02 0.02 0.02 0.02 0.02 0.02 0.02 0.02 0.02 0.02 0.02 0.02 0.02 0.02 0.02 0.02 0.02 0.02
8.1	0.563 0.566 0.567 0.567 0.566 0.565 0.564 0.563 0.562 0.561 0.560 0.559 0.558 0.557 0.556 0.555 0.554 0.553 0.02 0.02 0.02 0.02 0.02 0.02 0.02 0.02 0.02 0.02 0.02 0.02 0.02 0.02 0.02 0.02 0.02 0.02
8.2	0.570 0.573 0.574 0.574 0.573 0.572 0.571 0.570 0.569 0.568 0.567 0.566 0.565 0.564 0.563 0.562 0.561 0.560 0.02 0.02 0.02 0.02 0.02 0.02 0.02 0.02 0.02 0.02 0.02 0.02 0.02 0.02 0.02 0.02 0.02 0.02
8.3	0.577 0.580 0.581 0.581 0.580 0.579 0.578 0.577 0.576 0.575 0.574 0.573 0.572 0.571 0.570 0.569 0.568 0.567 0.02 0.02 0.02 0.02 0.02 0.02 0.02 0.02 0.02 0.02 0.02 0.02 0.02 0.02 0.02 0.02 0.02 0.02
8.4	0.584 0.587 0.588 0.588 0.587 0.586 0.585 0.584 0.583 0.582 0.581 0.580 0.579 0.578 0.577 0.576 0.575 0.574 0.02 0.02 0.02 0.02 0.02 0.02 0.02 0.02 0.02 0.02 0.02 0.02 0.02 0.02 0.02 0.02 0.02 0.02
8.5	0.591 0.594 0.595 0.595 0.594 0.593 0.592 0.591 0.590 0.589 0.588 0.587 0.586 0.585 0.584 0.583 0.582 0.581 0.02 0.02 0.02 0.02 0.02 0.02 0.02 0.02 0.02 0.02 0.02 0.02 0.02 0.02 0.02 0.02 0.02 0.02
8.6	0.598 0.601 0.602 0.602 0.601 0.600 0.599 0.598 0.597 0.596 0.595 0.594 0.593 0.592 0.591 0.590 0.589 0.588 0.02 0.02 0.02 0.02 0.02 0.02 0.02 0.02 0.02 0.02 0.02 0.02 0.02 0.02 0.02 0.02 0.02 0.02
8.7	0.605 0.608 0.609 0.609 0.608 0.607 0.606 0.605 0.604 0.603 0.602 0.601 0.600 0.599 0.598 0.597 0.596 0.595 0.02 0.02 0.02 0.02 0.02 0.02 0.02 0.02 0.02 0.02 0.02 0.02 0.02 0.02 0.02 0.02 0.02 0.02
8.8	0.612 0.615 0.616 0.616 0.615 0.614 0.613 0.612 0.611 0.610 0.609 0.608 0.607 0.606 0.605 0.604 0.603 0.602 0.02 0.02 0.02 0.02 0.02 0.02 0.02 0.02 0.02 0.02 0.02 0.02 0.02 0.02 0.02 0.02 0.02 0.02
8.9	0.619 0.622 0.623 0.623 0.622 0.621 0.620 0.619 0.618 0.617 0.616 0.615 0.614 0.613 0.612 0.611 0.610 0.609 0.02 0.02 0.02 0.02 0.02 0.02 0.02 0.02 0.02 0.02 0.02 0.02 0.02 0.02 0.02 0.02 0.02 0.02
9.0	0.626 0.629 0.630 0.630 0.629 0.628 0.627 0.626 0.625 0.624 0.623 0.622 0.621 0.620 0.619 0.618 0.617 0.616 0.02 0.02 0.02 0.02 0.02 0.02 0.02 0.02 0.02 0.02 0.02 0.02 0.02 0.02 0.02 0.02 0.02 0.02
9.1	0.633 0.636 0.637 0.637 0.636 0.635 0.634 0.633 0.632 0.631 0.630 0.629 0.628 0.627 0.626 0.625 0.624 0.623 0.02 0.02 0.02 0.02 0.02 0.02 0.02 0.02 0.02 0.02 0.02 0.02 0.02 0.02 0.02 0.02 0.02 0.02
9.2	0.640 0.643 0.644 0.644 0.643 0.642 0.641 0.640 0.639 0.638 0.637 0.636 0.635 0.634 0.633 0.632 0.631 0.630 0.02 0.02 0.02 0.02 0.02 0.02 0.02 0.02 0.02 0.02 0.02 0.02 0.02 0.02 0.02 0.02 0.02 0.02
9.3	0.647 0.650 0.651 0.651 0.650 0.649 0.648 0.647 0.646 0.645 0.644 0.643 0.642 0.641 0.640 0.639 0.638 0.637 0.02 0.02 0.02 0.02 0.02 0.02 0.02 0.02 0.02 0.02 0.02 0.02 0.02 0.02 0.02 0.02 0.02 0.02
9.4	0.654 0.657 0.658 0.658 0.657 0.656 0.655 0.654 0.653 0.652 0.651 0.650 0.649 0.648 0.647 0.646 0.645 0.644 0.02 0.02 0.02 0.02 0.02 0.02 0.02 0.02 0.02 0.02 0.02 0.02 0.02 0.02 0.02 0.02 0.02 0.02
9.5	0.661 0.664 0.665 0.665 0.664 0.663 0.662 0.661 0.660 0.659 0.658 0.657 0.656 0.655 0.654 0.653 0.652 0.651 0.02 0.02 0.02 0.02 0.02 0.02 0.02 0.02 0.02 0.02 0.02 0.02 0.02 0.02 0.02 0.02 0.02 0.02
9.6	0.668 0.671 0.672 0.672 0.671 0.670 0.669 0.668 0.667 0.666 0.665 0.664 0.663 0.662 0.661 0.660 0.659 0.658 0.02 0.02 0.02 0.02 0.02 0.02 0.02 0.02 0.02 0.02 0.02 0.02 0.02 0.02 0.02 0.02 0.02 0.02
9.7	0.675 0.678 0.679 0.679 0.678 0.677 0.676 0.675 0.674 0.673 0.672 0.671 0.670 0.669 0.668 0.667 0.666 0.665 0.02 0.02 0.02 0.02 0.02 0.02 0.02 0.02 0.02 0.02 0.02 0.02 0.02 0.02 0.02 0.02 0.02 0.02
9.8	0.682 0.685 0.686 0.686 0.685 0.684 0.683 0.682 0.681 0.680 0.679 0.678 0.677 0.676 0.675 0.674 0.673 0.672 0.02 0.02 0.02 0.02 0.02 0.02 0.02 0.02 0.02 0.02 0.02 0.02 0.02 0.02 0.02 0.02 0.02 0.02
9.9	0.689 0.692 0.693 0.693 0.692 0.691 0.690 0.689 0.688 0.687 0.686 0.685 0.684 0.683 0.682 0.681 0.680 0.679 0.02 0.02 0.02 0.02 0.02 0.02 0.02 0.02 0.02 0.02 0.02 0.02 0.02 0.02 0.02 0.02 0.02 0.02
10.0	0.696 0.699 0.700 0.700 0.699 0.698 0.697 0.696 0.695 0.694 0.693 0.692 0.691 0.690 0.689 0.688 0.687 0.686 0.02 0.02 0.02 0.02 0.02 0.02 0.02 0.02 0.02 0.02 0.02 0.02 0.02 0.02 0.02 0.02 0.02 0.02

Table II. The Scattering Law for $C_{15}H_{16}$ (T = 17°C)

β	S(α,β) · 10³																		
0,25	α = 0,166 S = 3000±35	0,52 436±25	1,00 555 25	1,50 576 25															
0,35	0,10 251 22	0,19 238 30	0,25 265 11	0,50 267 15	0,62 295 18	0,81 253 12	0,97 260 15	1,35 429 15	1,60 357 12	1,73 356 12	2,40 290 14	2,57 339 12							
0,45	0,12 140 15	0,23 184 50	0,28 223 12	0,48 236 30	0,65 250 20	0,89 247 12	1,15 250 40	1,65 275 9	1,72 304 12	2,45 290 9	2,54 304 12								
0,55	0,15 121 14	0,29 170 9	0,32 142 12	0,84 168 7	0,96 191 12	1,56 205 6	1,84 222 9	2,30 208 6	2,70 209 9										
0,65	0,17 78 11	0,20 135 23	0,35 141 10	0,44 112 7	0,50 128 5	0,80 110 8	1,04 142 12	1,43 148 6	1,68 165 4	1,95 159 10	2,10 139 9	2,76 161 7	2,87 167 12	3,30 162 2	4,10 129 6	4,90 154 4			
0,75	0,195 68 12	0,21 71 10	0,40 74 12	0,48 78 6	0,505 91 6	1,09 123 12	1,49 122 6	1,63 110 4	2,03 141 10	2,85 123 6	2,97 147 10	3,18 131 3	4,07 95 6	4,72 134 4					
0,85	0,22 64 10	0,235 95 12	0,52 66 5	1,15 104 10	1,60 85 4	2,12 127 8	3,08 112 2	4,56 122 4											
0,95	0,25 50 8	0,47 43 12	0,55 56 4	0,73 81 6	1,23 93 10	1,58 85 10	2,21 120 8	2,48 122 8	2,97 91 2	3,02 101 5	3,21 111 8	4,36 100 3	4,46 89 6	4,86 86 2	7,25 73 5				
1,10	0,31 51 8	0,56 50 4	0,59 62 5	0,80 59 3	0,99 76 4	1,32 77 6	1,68 77 4	1,93 55 3	2,36 82 5	2,60 114 3	2,82 73 2	3,17 76 4	3,48 84 4	4,15 83 2	4,65 71 9	4,90 69 2	6,88 60 2	7,50 64 2	10,28 46 2
1,30	0,35 44 5	0,65 49 3	0,86 41 4	1,00 52 3	1,46 65 8	1,50 46 2	1,79 64 4	2,57 59 6	2,67 55 1	2,73 83 3	3,34 70 4	3,41 42 2	3,95 61 2	4,89 61 5	5,28 56 2	6,70 49 1	7,84 49 3	10,00 41 2	
1,50	0,40 39 5	0,73 45 4	0,80 34 5	0,91 39 4	1,02 36 3	1,48 30 3	1,96 47 8	1,92 52 4	2,40 43 2	2,71 55 6	2,83 72 3	3,33 46 2	3,40 50 2	3,53 58 4	3,86 63 6	5,14 51 4	5,45 49 2	5,48 45 1	8,06 44 3	9,62 36 1
1,70	0,44 32 6	0,49 50 9	0,83 49 4	0,98 35 4	1,05 30 2	1,82 42 6	2,06 60 4	2,94 58 3	3,06 47 6	3,27 40 2	3,74 52 4								
1,90	0,50 37 5	0,59 29 9	0,94 42 4	1,04 32 3	1,08 24 2	1,97 34 6	2,03 44 4	3,06 53 3	3,20 33 2	3,26 39 6	3,98 42 4	4,55 42 5	5,73 38 3	5,80 37 2	6,10 38 1	8,55 34 3	8,95 30 1		
2,10	0,54 24 5	0,58 24 6	0,72 44 9	1,08 47 5	1,12 26 3	1,79 26 2	2,43 41 4	3,13 32 2	3,19 32 2	3,26 45 4	4,51 37 2	5,87 32 1	6,01 35 2	6,10 30 3	8,61 29 2	8,75 27 1	8,82 36 3	13,00 16 1	
2,30	0,60 19 6	0,66 32 5	1,15 20 9	1,18 27 2	1,21 20 4	1,42 25 2	2,14 42 6	3,05 32 2	3,33 45 2	3,43 42 5	4,44 33 26	4,84 52 5	5,66 31 1	6,20 24 2	8,28 20 1	8,75 18 1	9,12 30 2	12,67 16 2	
2,50	0,66 23 4	0,76 37 5	0,86 37 9	1,29 35 10	1,31 22 4	1,45 23 2	2,15 41 5	2,65 43 3	3,04 30 2	3,48 34 3	3,76 43 5	4,37 29 2	4,50 35 3	5,17 34 5	5,48 20 1	6,48 25 4	7,90 24 1	8,34 17	9,43 22 3	12,3 12 3
2,70	α = 0,72 S = 16 3	0,90 35 5	1,36 26 2	1,42 21 4	1,49 19 2	1,99 20 1	2,59 25 3	3,01 29 2	3,66 29 3	4,07 33 5	4,31 27 3	5,27 26 1	5,55 42 5	6,62 17 1	6,71 24 2	7,53 26 1	8,17 18 1	9,77 27 3	12,0 14 2	12,95 11 1	19,2 7 1
2,90	0,78 27 5	1,05 28 4	1,44 36 4	1,47 22 2	1,53 18 2	2,82 27 3	3,00 24 2	4,26 25 2	4,94 34 3	5,07 23 1	6,96 21 3	7,15 21 1	8,00 16 1	11,7 15 1					
3,10	0,79 13 3	0,89 16 4	1,54 26 5	1,60 16 2	1,63 20 2	1,83 13 8	2,03 12 1	2,97 25 6	3,00 21 2	3,80 29 3	4,20 24 2	4,52 25 5	4,68 20 1	5,97 30 5	6,55 15 1	6,70 27 1	6,99 20 2	7,75 16 1	10,13 19 2	11,3 15 1	12,73 10 1	18,91 5 1
3,30	0,84 7 3	1,00 16 5	1,26 37 10	1,67 21 2	2,07 12 1	3,03 20 2	3,24 24 2	3,31 12 1	4,05 24 3	4,15 29 1	4,68 18 1	5,27 22 3	5,30 29 1	6,47 12 1	7,29 18 2	7,50 20 3	7,54 15 1	10,9 15 1	10,53 21 2	11,60 5,9 0,4	12,48 8,8 0,5	18,49 6,5 0,7	23,14 2,5 0,2	34,59 1,0 0,2
3,50	0,93 11 2	1,08 16 5	1,73 16 1	2,05 19 4	2,10 9,7 1,0	3,08 17 3	4,12 15 1	4,48 19 1	5,90 11 1	6,37 13 1	7,38 14 1	10,60 14 2	10,21 8 1	16,0 5 1					
3,70	0,99 64 2	1,23 24 5	1,52 39 10	1,84 12 1	1,97 25 5	2,13 9 1	3,62 23 3	4,10 20 1	4,29 22 4	5,87 25 4	6,30 12 1	7,16 13 1	7,62 14 1	8,12 11 3	10,7 14 1	11,0 13 2	12,0 21 1	17,7 5 1					
3,90	1,09 9 5	1,47 11 2	4,01 16 2	6,95 12 1	9,82 12 1														
4,20	1,16 9 2	1,66 10 5	3,18 10 2	2,24 6 1	3,33 7 1	4,08 10 1	4,34 12 4	6,20 8 1	6,06 9 1	7,98 13 2	9,25 10 1	11,4 5 1	11,4 9 2	11,6 7 1	17,0 5 1	22,4 2,3 0,2	33,4 1,1 0,2		
4,60	1,33 6,1 1,7	2,35 6,2 0,7	3,36 4,8 0,6	4,83 14 4	6,08 8,5 0,6	8,38 9,0 2,0	11,1 3,6 0,2	11,2 5,6 0,7	11,9 7,2 2,1	16,3 4,5 0,3	21,7 2,0 0,1	32,3 1,0 0,1							
5,00	1,56 5,9 1,3	2,50 4,8 0,3	5,15 11 5	6,02 5,9 0,4	8,82 9 2	10,8 4,9 0,2	12,5 10 2	15,5 4,2 0,2											
5,40	1,83 5,6 1,3	2,73 5,1 1,6	3,43 3,1 0,6	5,95 4,2 0,5	10,3 4,3 0,2	10,9 2,8 0,2	14,8 3,6 0,2	21,1 1,3 0,1	31,3 1,0 0,1										
5,80	2,17 4,0 1,0	2,98 3,7 0,5	3,50 2,3 0,4	5,92 3,2 0,4	9,90 3,6 0,2	10,7 1,9 0,2	14,0 3,5 0,2	20,6 1,3 0,1	30,4 0,7 0,1										
6,20	2,42 4,3 1,0	3,60 3,4 0,4	5,95 3,2 0,4	9,50 2,8 0,2	10,6 1,5 0,2	12,1 3,0 0,2	20,1 1,0 0,1	29,6 0,8 0,1											
6,60	3,05 3,8 1,1	3,69 3,7 0,3	6,00 2,5 0,4	9,15 2,4 0,2	10,4 1,5 0,1	12,3 2,1 0,2	19,6 0,9 0,1	29,8 0,5 0,1											
7,00	3,75 3,2 0,2	6,17 3,0 0,3	8,73 2,1 0,3	11,6 1,9 0,3															

7,40	α = 3,85 S = 69±2	10,3 104 7	19,1 89 5	27,9 53 6
7,80		4,02 792±30	10,16 990 10	19,75 609 6
8,50		4,26 661±13	10,05 652 5	17,97 393 3
9,50		4,85 615±10	9,94 514 4	16,08 352 2
10,50		5,62 352±7	9,95 356 3	15,89 274 2
11,50		6,89 274±7	10,25 307 3	14,94 201 2